TECHNICAL REPORT n. 74

GAIA PERFORMANCE ON BRIGHT STARS

Daniele Gardiol, Deborah Busonero, Mario Gai, M.Lattanzi

Osservatorio Astronomico di Torino

GAIA performance on bright stars

1. Introduction

The data acquisition and reduction of bright stars with Gaia requires particular care in the definition of hardware and/or software processing due to the saturation of the CCD dynamical range and the corresponding impact on limiting magnitude. With the current specifications and in normal operation mode, stars of magnitude $V \cong 12 mag$ saturate the ASTRO CCDs.

Historically, two solutions have been proposed to overcome this limit and expand the lower magnitude limit in order to allow Gaia to perform high precision measurements on bright objects, thus obtaining relevant scientific results in very important fields of modern astronomy:

- Wing method: saturation is avoided by adapting the readout window shape to the star magnitude, taking data from the wings of the PSF rather than from the saturated core.
- Gate method: saturation is eliminated by reducing the on-chip integration time according to the bright star magnitude, when it enters the CCD field.

For our purposes, a "window" is the spatial region for which CCD data are acquired and stored.

The astrometric performances of Gaia on bright stars and the comparison between the two methods have been the subjects of a dedicated note in the past[1].

More recently the option of unbinned pixel readout in the case of bright stars has been proposed[2].

Purpose of this document is to describe the results of simulations performed to estimate the astrometric error at the level of one single CCD transit. This is done for different possible operation options, including readout modes, windowing schemes and centring algorithms.

2. Source characteristic

A solar star with spectral type G2V is used as reference source, simulated in first approximation by a black body emission profile.

3. Environmental parameters

The main parameters used in the simulation and their value are shown in Table 1. They are derived from the Gaia Parameter Database on the Gaia livelink site.

Parameter	Value	Notes
Telescope focal length	46700 mm	
Telescope aperture size	1400 x 500 mm²	Two identical telescopes
Total optical transmissivity	See Figure 1	Single reflection
Integration time on-chip	3.312 s	Single CCD transit
CCD quantum efficiency	See Figure 1	
CCD total detection noise	16 el/pixel	Includes RON, Dark, KTC, video chain
CCD charge handling capacity	3,5 10^5 el	Readout register, ideal saturation
CCD full well capacity	1,9 10^5 el	Image portion of the CCD
CCD pixel size	10 x 30 μm	Respectively along and across scan

Table 1 – Parameters used in the simulation

INAF – Osservatorio Astronomico di Torino, strada Osservatorio 20, 10025 Pino Torinese – Torino
tel. +39 011 8101900, fax: +39 01 8101930

4. Point Spread Function

4.1 Optics

Optical aberrations and chromatic effects are introduced by means of the Zernike polynomials description of the Wavefront Error (WFE). We built a detailed representation of the baseline configuration[3] and derived the Wavefront characteristics for a sample of representative points in the Field of View. We are therefore able to simulate a Point Spread Function for a given point in the Field of View that describes all the aberrations introduced by the telescope optical train. In this way all the aberrations that contributes to the error budget are naturally introduced and taken into account.

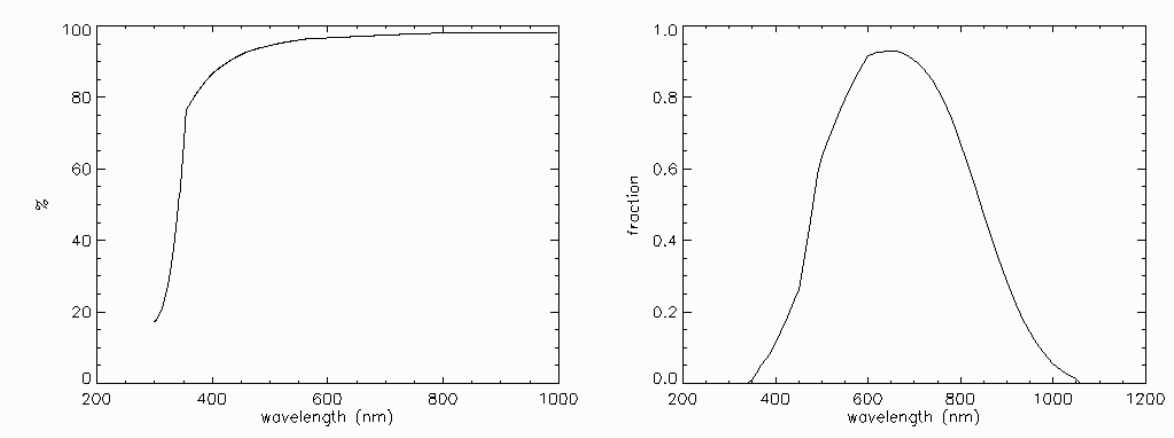

Figure 1 – Single mirror reflectivity (left) and CCD quantum efficiency (right)

4.2 CCD Effects

The PSF degradation due to finite pixel size is included in the model implementation.
Effects such those introduced by TDI scan are currently not taken into account, as not considered dominant. Pixel MTF will be introduced in a future step.

4.3 Saturation

Ideal saturation is implemented, i.e. each pixel behaves linearly up the saturation limit, which is a) the *full well capacity* ($1{,}9 \cdot 10^5$ electrons) for the image section of the CCD or b) the *charge handling capacity* ($3{,}5 \cdot 10^5$ electrons) for the readout register. After that, the pixel is considered saturated.

4.4 Gates

Gates principle is described in an Astrium document[1]. Quoting directly from there: «The method for varying the number of pixel rows over which the TDI function is obtained, i.e. length selection, is as follows. Down each inter-column isolation structure is a drain of the type normally used for anti-blooming purposes. At 12 locations down the image section are separately connected Image clock electrodes, designated TDn with n between 1 and 12. These electrodes are normally clocked with the image clocks but any one of them can be held at a suitably low constant voltage in order to block charge transfer down the array. Signal charge transferred towards the selected electrode then accumulates under the electrodes of the preceding pixel and any charge in excess of the full-well capacity is lost to the drain. The TDI length is thus the remaining number of pixels in the image section following the selected gate.».

In the current design, twelve gates are implemented according to Table 2.

INAF – Osservatorio Astronomico di Torino, strada Osservatorio 20, 10025 Pino Torinese – Torino
tel. +39 011 8101900, fax: +39 01 8101930

TDI number	1	2	3	4	5	6	7	8	9	10	11	12
TDI lengths (pixels)	2	4	8	16	32	64	128	256	512	1024	2048	2900
Exp. Time (s)	0.0015	0.0029	0.0059	0.0117	0.0235	0.0469	0.0939	0.1877	0.3755	0.7509	1.5019	2.1267

Table 2 – TDI lenghts and Exposure Times for the twelve gates implemented

The total length of the image area with no gate selected is 4496 pixels, corresponding to an integration time of 3.312 seconds.
Figure 2 gives a graphic representation of the position of some Gates on the CCD; gate numbers below 7 are not visible on this scale.

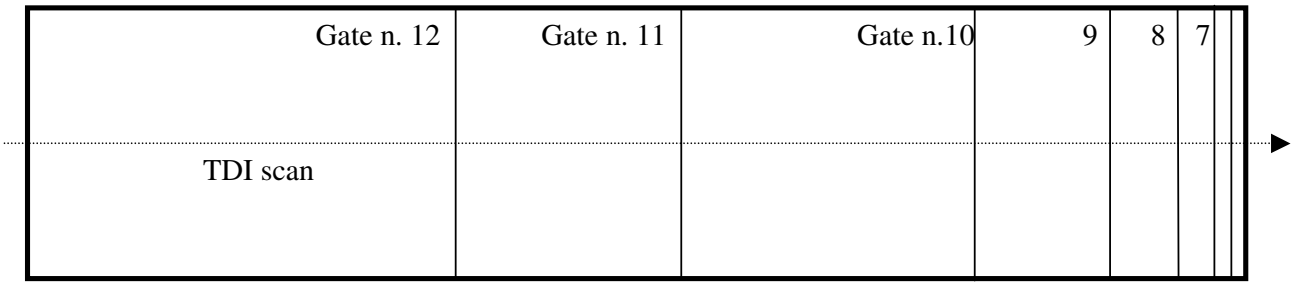

Figure 2 – Position of gates 7 to 12 on the CCD

5. Image processing

5.1 Windowing

Size and type of windows on ASTRO CCDs AF2-10 depends on the star magnitude. Currently, the proposed readout scheme for stars brighter than $G = 16 mag$ is a window size of 12x12 px². For stars brighter than $G = 12 mag$ the whole 12x12 pixel window is transmitted (WAP, see reference 2), while for fainter stars ($G > 12 mag$) the window is binned on chip in the across scan direction (WA2R12, see again reference 2), and the size of the transmitted window is 12 x 1 px². In this document, the former readout scheme is referred to as UnBinned or full resolution case, whereas the latter will be named Binned. The readout schemes will be used over a magnitude range wider than originally intended to compare the potential performance.

5.2 Location algorithm

A comparison between two different algorithms is implemented:
a) determination of the star position by comparison of the measured PSF with the nominal template, using a least square approach (LSA);
b) simple centre of gravity (COG) or barycentre.

6 Simulation approach

The evaluation is based on a Montecarlo approach. For each magnitude, within a given magnitude range, we build a sample of detected PSF instances, including realistic noise. For each instance within the sample we compute the star position with the two algorithms, obtaining therefore two values of star position; from each sample, mean position and standard deviation are derived. The size of the sample is 900 instances.
The nominal phase between the PSF and the CCD pixel array is fixed to zero.

INAF – Osservatorio Astronomico di Torino, strada Osservatorio 20, 10025 Pino Torinese – Torino
tel. +39 011 8101900, fax: +39 01 8101930

7 Results

7.1 Comparison between barycentre and least square algorithms – Binned readout

The results of the comparison between the COG and the LSA are summarised in Figure 3 (top panel). Four data sets are shown, over the magnitude range between about 11.5 and 15. Diamonds are related to the LSA, while asterisks refer to the COG. Both these simulations have been made using an aberrated PSF, and therefore represent a realistic case. The two lines show the simulation results deduced from a non-aberrated PSF (i.e. they represent the "ideal case", used as a sanity check) and are shown for comparison; the solid line refers to the LSA, while the dotted line refers to the COG. The parameters used for simulation are given in Table 3.

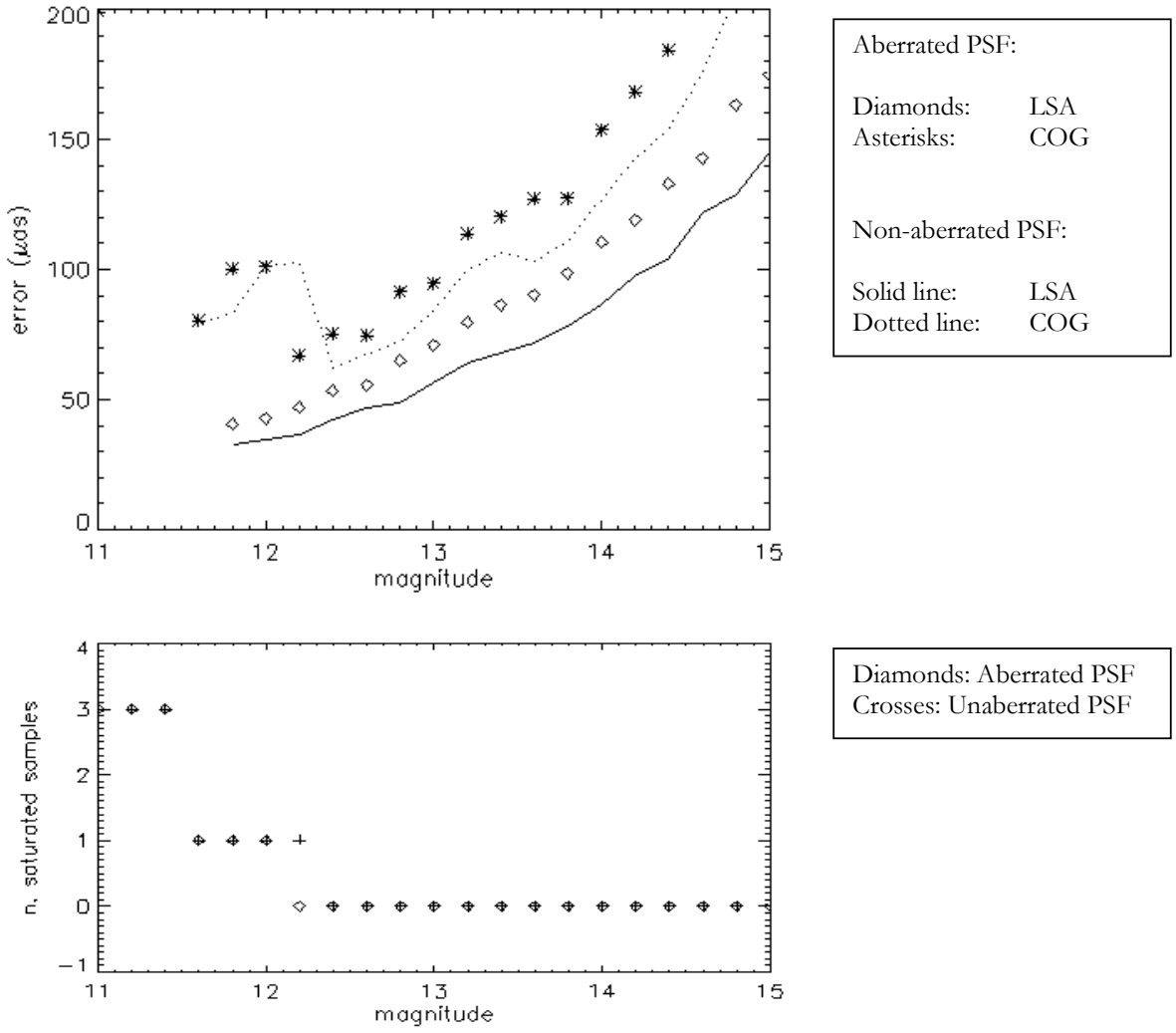

Figure 3 – Comparison between barycentre and least square algorithms

INAF – Osservatorio Astronomico di Torino, strada Osservatorio 20, 10025 Pino Torinese – Torino
tel. +39 011 8101900, fax: +39 01 8101930

Parameter	Value	Notes
PSF	Unaberrated Aberrated	(reported as lines) (reported as symbols)
Algorithm	COG LSA	(reported as asterisks and dotted line) (reported as diamonds and solid line)
Sample size	900	No phase shift between sample elements
Windowing	12 x 1 px²	Binned on chip in across scan direction No gates
Saturation	Yes, at 3,5 10^5 el	CCD linear until saturation occurs.

Table 3 – Simulation parameters for test 7.1

The bottom panel of Figure 3 shows the number of saturated samples vs. star magnitude. As expected, the realistic (aberrated) PSF has brighter saturation magnitude.
We are using for the whole magnitude interval the Binned windowing. Saturation of the PSF occurs at about G=12 for the aberrated PSF, while the unaberrated PSF saturates at about G=12.2. The difference is due to the fact that the aberrated PSF is "smoothed" by the optical aberrations, reducing the peak value, and therefore saturation occurs at slightly brighter magnitudes.
At the faint end of the magnitude range, it is possible to compare the results with the precision values obtained with the performance evaluation for the Gaia baseline and alternative configurations. The values (of order of 200 μas) are consistent, within the approximations.
In both aberrated and non aberrated cases, the LSA shows better performance than the COG, as expected. The dispersion of position estimates is smaller, and in agreement with the known nominal position of the star, for the LSA, while the COG shows larger errors and a relevant bias (not shown in the figure) due to the value of the phase shift between the PSF and the position of the CCD pixel array.
When saturation of the brightest pixel occurs, the COG shows a significant degradation of the astrometric accuracy, which might be associated to the loss in signal to noise ratio. The same does not hold for the LSA, which, despite the loss of photons, seems to be practically unaffected by saturation. The LSA estimation of the star position is still good in the non aberrated case, while in the aberrated one there is a small systematic error, apparently increasing at brighter magnitudes. One possible explanation is related to the asymmetry of the PSF, that could introduce higher order effects when saturation occurs. Another possibility is that the effect is due to the algorithm implementation. In any case, this effect suggests the need for further optimisations.
From now on we will abandon the COG algorithm and will focus on the optimisation of the LSA in the saturated region. The results will be compared with the proposed gate readout method.

7.2 Improved LSA algorithm

Figure 4 (top panel) shows the result on astrometric precision obtained after numerical improvements of the algorithm. The bottom panel again shows the number of saturated pixels.
The results of the improved algorithm are shown as a solid line, which is compared with some of the results from the previous section. The behaviour of the improved algorithm is consistent with the previous LSA results for magnitudes fainter than about $G \cong 12 mag$, but now reliable and consistent results are obtained over a larger magnitude range, down to $G \cong 10 mag$, corresponding to a region with three saturated samples over a total of twelve. There is also a precision "jump" at the border regions affected by either 2 or 3 saturated samples. The general behaviour is a precision range of 30~60 μas over the magnitude range $G \cong 10-13 mag$.
COG and LSA on non-aberrated PSF are not extrapolated to the brighter magnitude range, as respectively undesirable and unrealistic in terms of performance.
The improved LSA (hereafter, ILSA) has also a much smaller systematic error.

INAF – Osservatorio Astronomico di Torino, strada Osservatorio 20, 10025 Pino Torinese – Torino
tel. +39 011 8101900, fax: +39 01 8101930

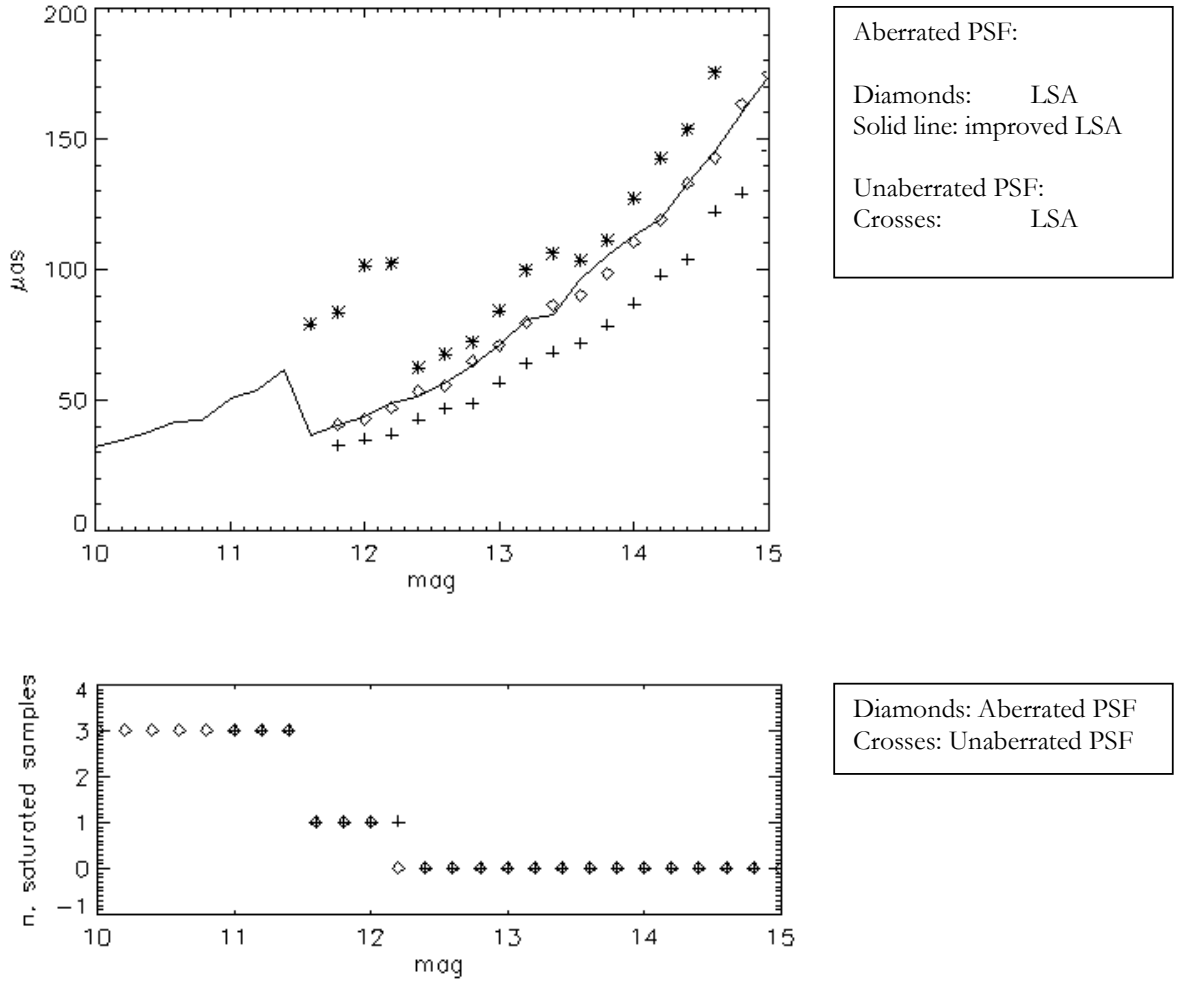

Figure 4 – Astrometric error with improved least square algorithm

7.3 Gates - Binned readout

The magnitudes of interest for the gates are those associated with PSF saturation. With the current configurations, for realistic (aberrated) PSFs, activation of the first gate (gate number 12) is required for magnitudes $G < 12 mag$. The results obtained with the parameters reported in Table 4 are summarised in Figure 5. In the top panel, we show the astrometric precision achieved by ILSA on the Binned readout data, either without gate usage (as in the previous test), represented by diamonds, or with the gates (solid line).

Each of the twelve gates (identified with number from 1 to 12, in order of increasing exposure time) allows operation over a magnitude range of about 0.8 mag. In this way, gate n. 1 allows to reach magnitude 4 without saturation of the CCD. For brighter magnitudes, even the use of the "shortest" TDI length induces saturation of the CCD.

As expected, the astrometric error has a saw-tooth behaviour, due to the activation of subsequent gates. In the bottom panel of Figure 5, we show both the number of saturated pixels without gate usage (diamonds), and the active gate number (asterisks).

INAF – Osservatorio Astronomico di Torino, strada Osservatorio 20, 10025 Pino Torinese – Torino
tel. +39 011 8101900, fax: +39 01 8101930

For realistic (aberrated) PSFs, the astrometric error is within the range [50,70] μas. A comparison with the non aberrated case shows a degradation of the astrometric error of about 20%.

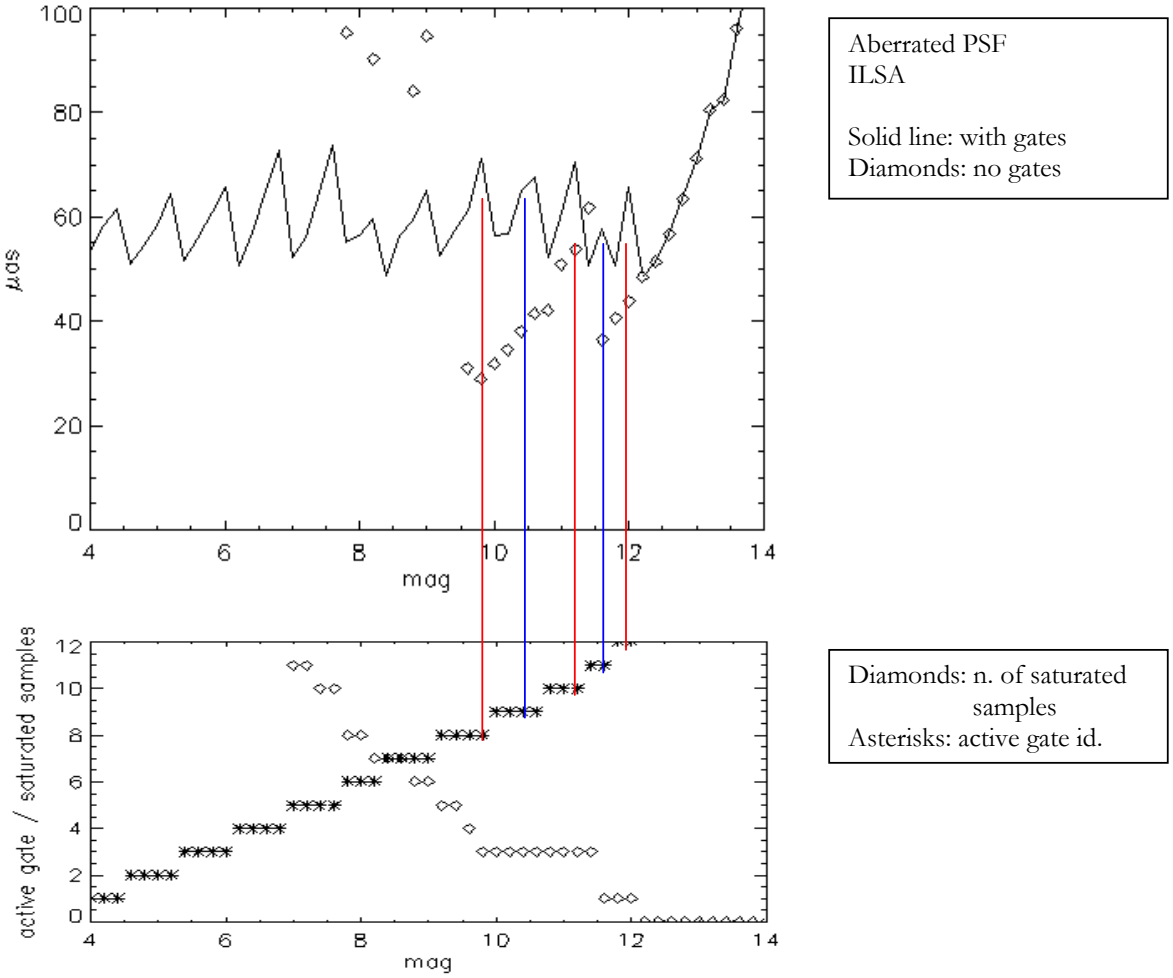

Figure 5 – Astrometric error with gates

Parameter	Value	Notes
PSF	Unaberrated Aberrated	(not shown) (line / diamonds)
Algorithm	ILSA	
Sample size	900	No phase shift between sample elements
Windowing	12 x 1 px²	Binned on chip in across scan direction Gates are active
Saturation	Yes, at 3,5 10^5 el	CCD linear until saturation occurs.

Table 4 – Simulation parameters for test 7.3

7.4 Gates – Binned vs. UnBinned readout

In this paragraph we report the results obtained with the UnBinned readout method. The simulation setup is the same of the previous paragraph, with two major changes:

INAF – Osservatorio Astronomico di Torino, strada Osservatorio 20, 10025 Pino Torinese – Torino
tel. +39 011 8101900, fax: +39 01 8101930

- The saturation level is now the full well capacity of the image section of the CCD;
- The readout implemented is the UnBinned full resolution windowing (identified by the WAP acronym, see paragraph 5.1).

In Table 5 we briefly recall the simulation parameters. Results are shown in the top panel of Figure 6 (dashed line), compared with the previous case of gates + Binned PSF (solid line).

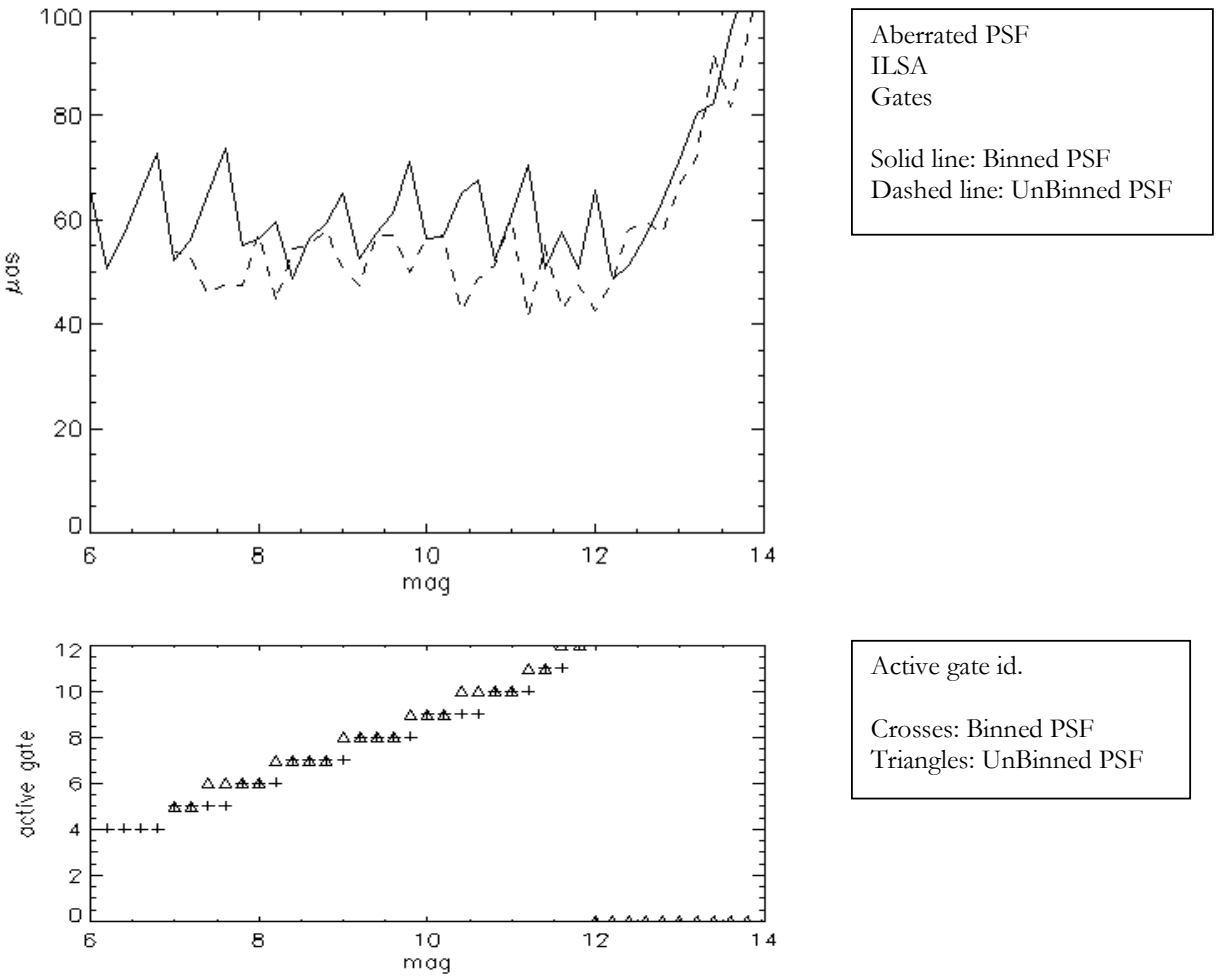

Figure 6 – Astrometric error with gates – comparison between Binned and UnBinned readout

The bottom panel of Figure 6 shows the gate activation by either Binned (crosses) and UnBinned (triangles) readout. From a comparison of the two panels, we see that

- the same gate is activated by UnBinned readout about 0.3 magnitudes brighter than Binned readout;
- The UnBinned PSFs astrometric error shows an average improvement of ~10-15%.

It can be shown that this results are consistent with an analytical PSF model based on classical Fresnel diffraction.

Parameter	Value	Notes
PSF	Aberrated	
Algorithm	ILSA	
Sample size	900	No phase shift between sample elements

INAF – Osservatorio Astronomico di Torino, strada Osservatorio 20, 10025 Pino Torinese – Torino
tel. +39 011 8101900, fax: +39 01 8101930

Windowing	12 x 12 px²	UnBinned PSF (dashed line) Binned PSF (solid line) shown for comparison Gates are active
Saturation	Yes, at 1,9 10^5 el	CCD linear until saturation occurs

Table 5 – Simulation parameters for test 7.4

7.5 Performance variation over field of view

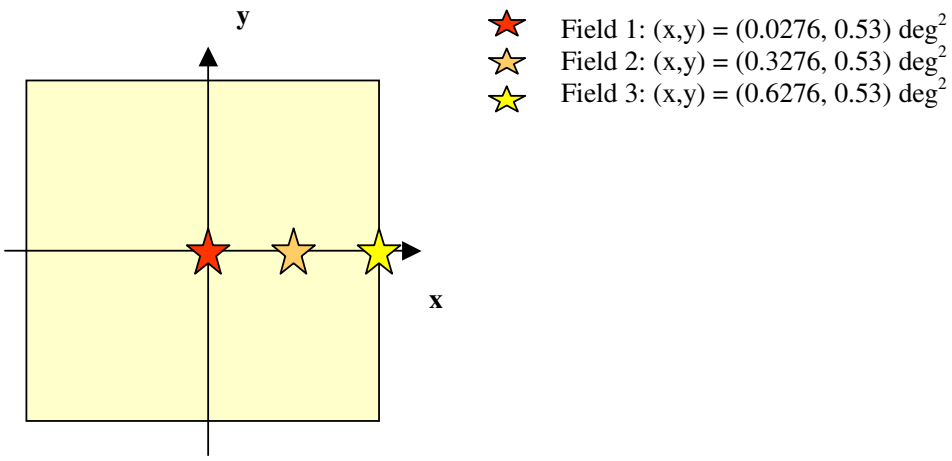

Figure 7

The analysis of the performance variation over the field of view (FOV) is limited in this example to three points shown in Figure 7. They have the same along scan coordinate, on the axis of symmetry of the field of view, and have different across scan coordinates. They represent therefore different objects in transit at different across scan positions on the detector. Even if the sample is limited, the results give interesting information.
We consider two cases, with or without gate activation.
The case when gates are active is shown in Figure 8:

- there is evidence of a significant field dependence, due to the different PSF/CCD phase shift;
- the overall trend is nevertheless similar for the three field positions;
- the performance is in the range 40-70 μas for G ~ 8-12 mag.

The results of previous tests are thus confirmed over the FOV.

INAF – Osservatorio Astronomico di Torino, strada Osservatorio 20, 10025 Pino Torinese – Torino
tel. +39 011 8101900, fax: +39 01 8101930

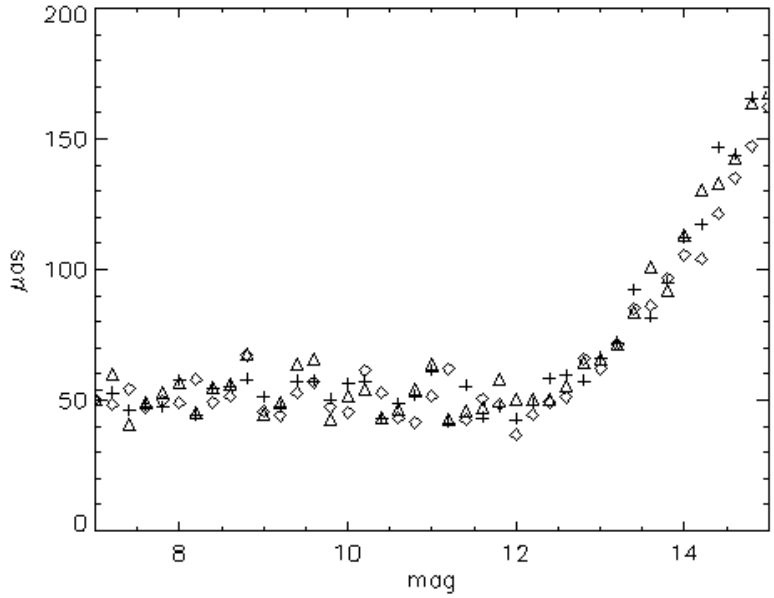

Crosses: Field position n.1
Diamonds: Field pos. n.2
Triangles: Field position n.3

Figure 8 – Performance variation over the field of view – Gates are active

The performance in the case without gates is shown in Figure 9 (top panel):

- there is evidence of a significant field dependence, due again to the different PSF/CCD phase shift;
- the performance is highly degraded below G ~ 10 mag;
- the performance is between 30 ~60 μas for G ~ 10-12 mag (two over three cases).

The case with significant degradation in the range G ~ 10-12 mag has an higher number of saturated pixels, as shown in Figure 9 (bottom panel); besides, it reaches the 30 μas error level for fainter magnitudes.

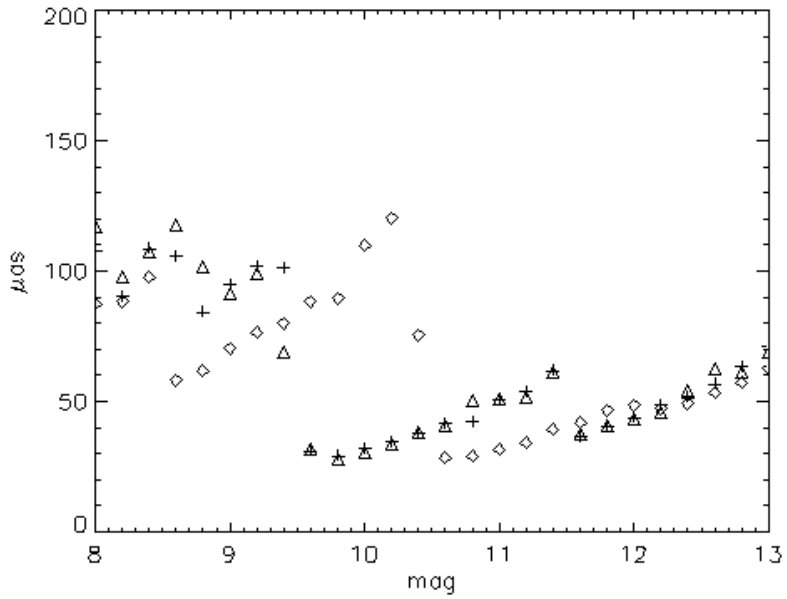

Crosses: Field position n.1
Diamonds: Field pos. n.2
Triangles: Field position n.3

INAF – Osservatorio Astronomico di Torino, strada Osservatorio 20, 10025 Pino Torinese – Torino
tel. +39 011 8101900, fax: +39 01 8101930

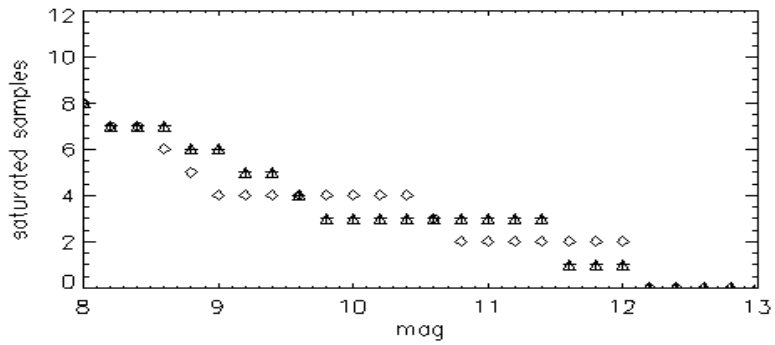

Figure 9 – Performance variation over the field – without gates

7.6 Binning vs. full resolution

Figure 10 shows a comparison of the astrometric error obtained with the different readout methods investigated so far as a function of magnitude.

The best performance over the magnitude range $G = 10 - 11 mag$ and $G = 11.5 - 12 mag$ is obtained for the standard readout mode used for fainter stars (i.e. no gates, Binned across scan), but with a suitable, robust location algorithm, in spite of CCD saturation.

The use of full resolution readout is expected to improve precision, but requires a more robust location algorithm, currently under development. The expected result is a smoother distribution, with error of order of 35 μas over the whole magnitude range $G = 10 - 12 mag$, and comparable or lower error for brighter magnitudes.

It appears that the most convenient implementation of the gate option is such that partial saturation at the chip level is tolerated.

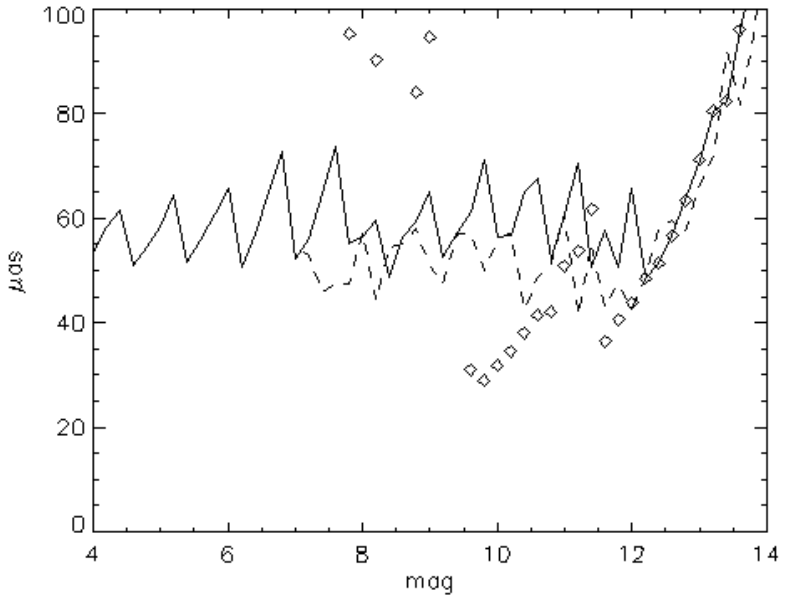

Figure 10

INAF – Osservatorio Astronomico di Torino, strada Osservatorio 20, 10025 Pino Torinese – Torino
tel. +39 011 8101900, fax: +39 01 8101930

8 Conclusions

Magnitude	No gates, Binned	Gates, Binned	Gates, UnBinned
12	45 μas	50-70 μas	45-65 μas
11	50 μas		
10	30 μas		
8	100 μas		
< 8	N/A		

Table 6

The readout scheme proposed for Gaia, and summarised as follows:

- on-chip binning to 6x1 samples of a 6x12 pixel window for $G > 16 mag$ stars;
- on-chip binning to 12x1 samples of a 12x12 pixel window for $12 mag \le G \le 16 mag$ stars;
- full resolution readout to 12x12 samples of a 12x12 pixel window for $G \le 12 mag$ stars;
- gate activation for sufficiently bright stars;

appears to be able to provide very good potential results on bright stars, with the following cautions:

a) An adequate location algorithm must be used; the most convenient appears to be the least square algorithm, with an appropriate implementation to take into account partial saturation of the detected samples.

b) The gate activation must NOT be selected under the constraint of retaining the whole detected signal within the useful dynamic range, but rather with the aim of limiting the saturated region to a manageable level.

The next developments planned in INAF-OATo consist in implementing the required robust least square algorithm for the full resolution, partial saturation case, in order to verify the current understanding and provide a more detailed, realistic, assessment of the Gaia CCD level astrometry on bright stars.

1 L.Gautret, "GAIA – Comparison of wings and gates", GAIASYS.NT.00096.T.ASTR, EADS Astrium
2 E.Hoeg, "Summary of Sampling Schemes for ASM, AF, BBP, SSM and MBP", GAIA-CUO-151
3 Gardiol D., Loreggia D., Mannu S., Mottini S., Perachino S., Gai M., Lattanzi M.G., "End-to-end opto-mechanical simulation for high precision global astrometry", proc. SPIE 5497, 2004, p. 461

INAF – Osservatorio Astronomico di Torino, strada Osservatorio 20, 10025 Pino Torinese – Torino
tel. +39 011 8101900, fax: +39 01 8101930